

We are IntechOpen, the world's leading publisher of Open Access books Built by scientists, for scientists

4,800

Open access books available

122,000

International authors and editors

135M

Downloads

Our authors are among the

154

Countries delivered to

TOP 1%

most cited scientists

12.2%

Contributors from top 500 universities



WEB OF SCIENCE™

Selection of our books indexed in the Book Citation Index
in Web of Science™ Core Collection (BKCI)

Interested in publishing with us?
Contact book.department@intechopen.com

Numbers displayed above are based on latest data collected.
For more information visit www.intechopen.com



Chapter

Comparative Study and Simulation of Different Maximum Power Point Tracking (MPPT) Techniques Using Fractional Control & Grey Wolf Optimizer for Grid Connected PV System with Battery

Mohamed Ahmed Ebrahim and R.G. Mohamed

Abstract

This chapter presents the comparative analysis between perturb & observe (P&O), incremental conductance (Inc Cond), and fractional open-circuit voltage (FOCV) algorithms using fractional order control & a new meta-heuristic called Grey Wolf optimizer (GWO) for extracting the maximum power from photovoltaic (PV) array. PV array systems are equipped with maximum power point tracking controllers (MPPTCs) to maximize the output power even in the case of rapid changes of the panel's temperature and irradiance. In this chapter, three cost effective MPPTCs are introduced: FOCV, P&O and Inc. Cond. The output voltage of the array is boosted up to a higher value so it can be interfaced to the local medium voltage distribution network.

Keywords: maximum power point tracking, grid connected photovoltaic, battery, grey wolf optimizer, boost converter, fractional order PI control

1. Introduction

Solar photovoltaic array system (SPVS) is one of the most prominent sources of electrical energy. SPVS is environmentally friendly and as a result there are no CO₂ emissions [1]. The energy dilemma represents in increasing the electricity production from the resources matching with the environment requires searching for new green, renewable, and sustainable ideas. SPVS along with wind turbines and fuel cells are possible innovative solutions for this dilemma [2, 3]. It was stated [4] that solar power capacity has expanded rapidly to 227 GW by the end of 2017 with a global growth rate of 26% which was higher than in 2016 (16.4%). Solar energy production was around 11% of the global renewable generation capacity, and increasing [4]. The installed capacity of SPVS in Egypt was about 1% of the total

electricity production from renewable energy sources in March 2018 [5]. In SPVSS, the operation at the maximum power point (MPP) is necessity. As a result for this, various MPP tracking (MPPT) techniques are developed, investigated and implemented in the last decades [6]. One of the most powerful techniques is the fractional order PID (FOPID) based MPPT controller (MPPTC) [7]. These kinds of controllers have merged the merits of classical MPPTCs and PID controller [8]. However, FOPID based MPPTCs require efficient tuning methods to improve the dynamic response especially in the presence of system disturbances [9]. Thanks to Meta heuristic optimization techniques that can be employed to significantly tune MPPTCs.

In this chapter, design methodology for three different types of MPPTCs using fractional order PID (FOPID) is summarized.

This chapter also presents a new meta-heuristic called Grey Wolf Optimizer (GWO) inspired by grey wolves. The GWO algorithm mimics the leadership hierarchy and hunting mechanism of grey wolves in nature. Three main steps of hunting, searching for prey, encircling prey, and attacking victim, are implemented in this algorithm [10].

2. Practical case study

This study present PV solar power plant connected to the Egyptian national grid and installed in Kom Ombo, Aswan, Egypt. This power plant will have a total capacity of 20 MW which can be considered one of largest Egyptian PV project. The PV system is constructed using MATLAB/SIMULINK to mimic the actual system. Different scenarios are considered to test the effectiveness of the proposed MPPTCs. These scenarios include small as well as large environmental conditions changes.

3. Proposed system simulation

The simulation of grid-connected PV system with battery contains various simulation blocks such as PV array, battery, battery charge controller, three-phase voltage source inverter, the filter circuit, load, utility grid, and MPPT. **Figure 1** shows proposed system simulation. PV array is connected to the 11-kV network via a DC-DC boost converter and a three-phase three-level voltage source converter (VSC). In this paper, PV array generates a voltage of 666 V DC for a solar irradiance

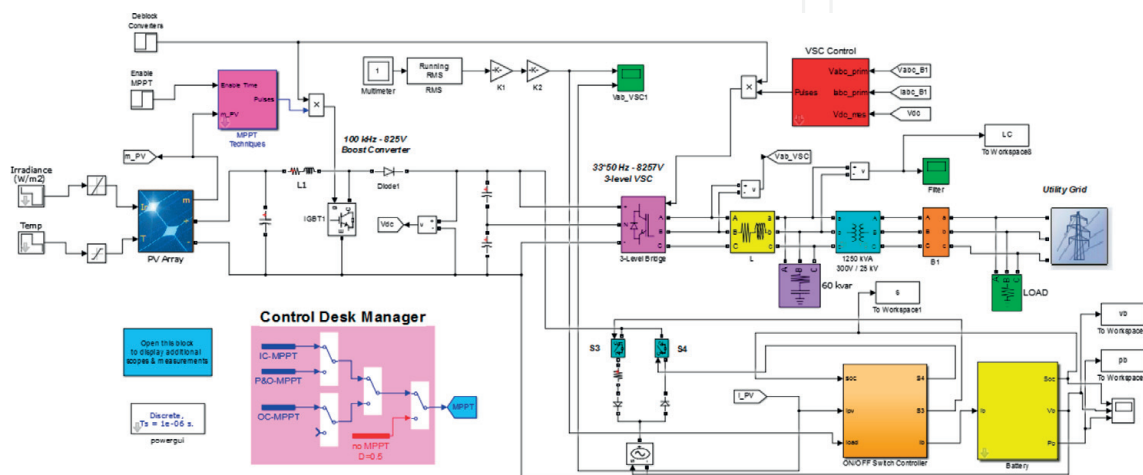


Figure 1.
Proposed system simulation.

of 1000 W/m². The 100-kHz DC-DC boost converter is increasing voltage from PV natural voltage (666 V DC at maximum power) to 825 V DC. Switching duty cycle is optimized by an MPPT controller that using different techniques such as ‘Incremental Conductance, Hill Climbing/Perturb and Observe (P&O), and Fractional Open-Circuit Voltage (VOC) techniques. This MPPT technique automatically varies the duty cycle to generate the required voltage to extract maximum power 1980-Hz 3-level 3-phase VSC. The VSC converts the 825 V DC link voltage to 300 VAC and keeps unity power factor.

4. Problem overview

The most challenging problem considered by PV array system is how to automatically maintain the operation at maximum output power under environmental conditions continuous variation. In this chapter, a power converter that can vary the current coming from the PV array is employed as illustrated in **Figure 2** [6]. **Figure 2** shows pulse width modulation based boost converter. The philosophy of operation of the converter depends on the on and off states of the switch S [11, 12]. The power converter (boost converter) parameters can be sized using the following equations [13]:

$$\frac{V_o}{V_g} = \frac{1}{1 - D} \quad (1)$$

$$L = \left(\frac{V_g * D}{f * CRF} \right) \quad (2)$$

$$R_o = \frac{V_o}{I_o} \quad (3)$$

$$C = \frac{D}{(f \times R_o \times VRF)} \quad (4)$$

where D is the duty cycle ratio, V_g is the input voltage to boost converter, V_o is the output voltage from boost converter, f is the switching frequency, VRF is voltage ripple factor (according to IEC harmonics standard, VRF should be bounded within 5%), CRF is the current ripple factor (according to IEC harmonics standard, CRF should be bounded within 30%) [14] and R_o is the load resistance. We introduce the different MPPT techniques below in an arbitrary order.

4.1 Incremental conductance algorithm

Inc. Cond based MPPTC is derived from the fact that there are three operating regions around MPP. Each operating region has unique characteristics represented

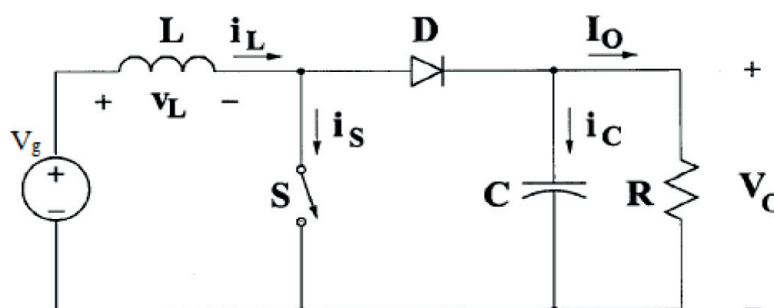


Figure 2.
 Circuit diagram of boost converter.

in the ratio between the power change and the voltage change. Roughly speaking, it can be considered that Inc. Cond based MPPTC is based on the slope of the PV array power curve [15, 16].

$$\begin{cases} \frac{dP}{dV} = 0, \text{ at MPP} \\ \frac{dP}{dV} > 0, \text{ left of MPP} \\ \frac{dP}{dV} < 0, \text{ right of MPP} \end{cases} \quad (5)$$

Since

$$\frac{dP}{dV} = \frac{d(IV)}{dV} = 1 + V \frac{dI}{dV} = 1 + V \frac{\Delta I}{\Delta V} \quad (6)$$

$$\begin{cases} \frac{\Delta I}{\Delta V} = -\frac{I}{V}, \text{ at MPP} \\ \frac{\Delta I}{\Delta V} > -\frac{I}{V}, \text{ left of MPP} \\ \frac{\Delta I}{\Delta V} < -\frac{I}{V}, \text{ right of MPP} \end{cases} \quad (7)$$

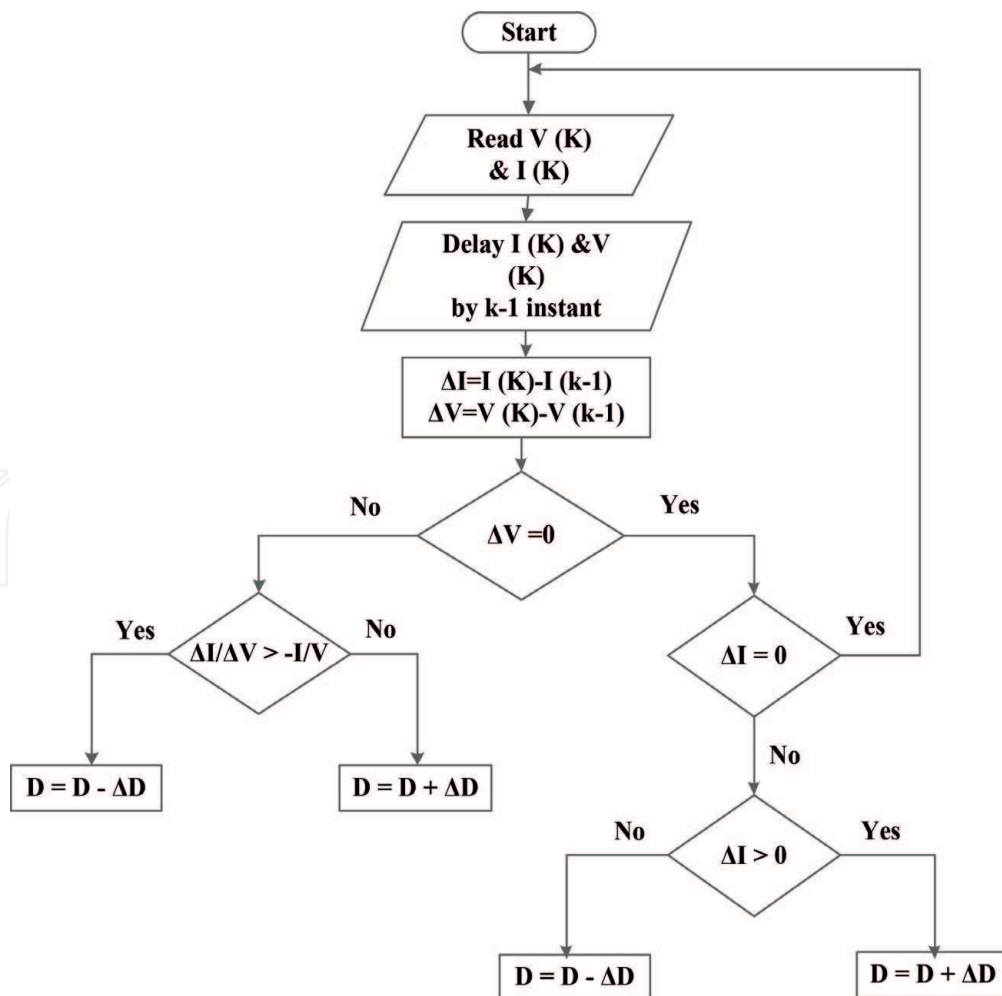


Figure 3. Incremental conductance MPPT flowchart used for MATLAB simulation.

Thus, MPP can be tracked by comparing the instantaneous conductance (I/V) to the incremental conductance ($\Delta I/\Delta V$) as shown in the flowchart illustrated in **Figure 3**. The algorithm decrements or increments the duty cycle to track the new MPP. The increment size determines how fast the MPP is tracked.

4.2 Hill climbing/P&O algorithm

According to the sign of dP/dV where dP is the difference between power and dV is the difference between voltage of two succeeded point Hill climbing involves a perturbation in the duty ratio of the power converter [15–17]. The flow chart of the algorithm is shown in **Figure 4**. It is observed from P-V characteristic curve of the solar PV module that there are three main regions for operation. The first region is at the right hand side of MPP where the ratio between the power change over the voltage change (dP/dV) is negative. The second region is at the left hand side of MPP where the ratio dP/dV is positive. Moreover, the third region is at MPP exactly where the ration dP/dV is zero. P&O based MPPTC decides whether to increase or decrease the duty cycle depending on these three regions of operation.

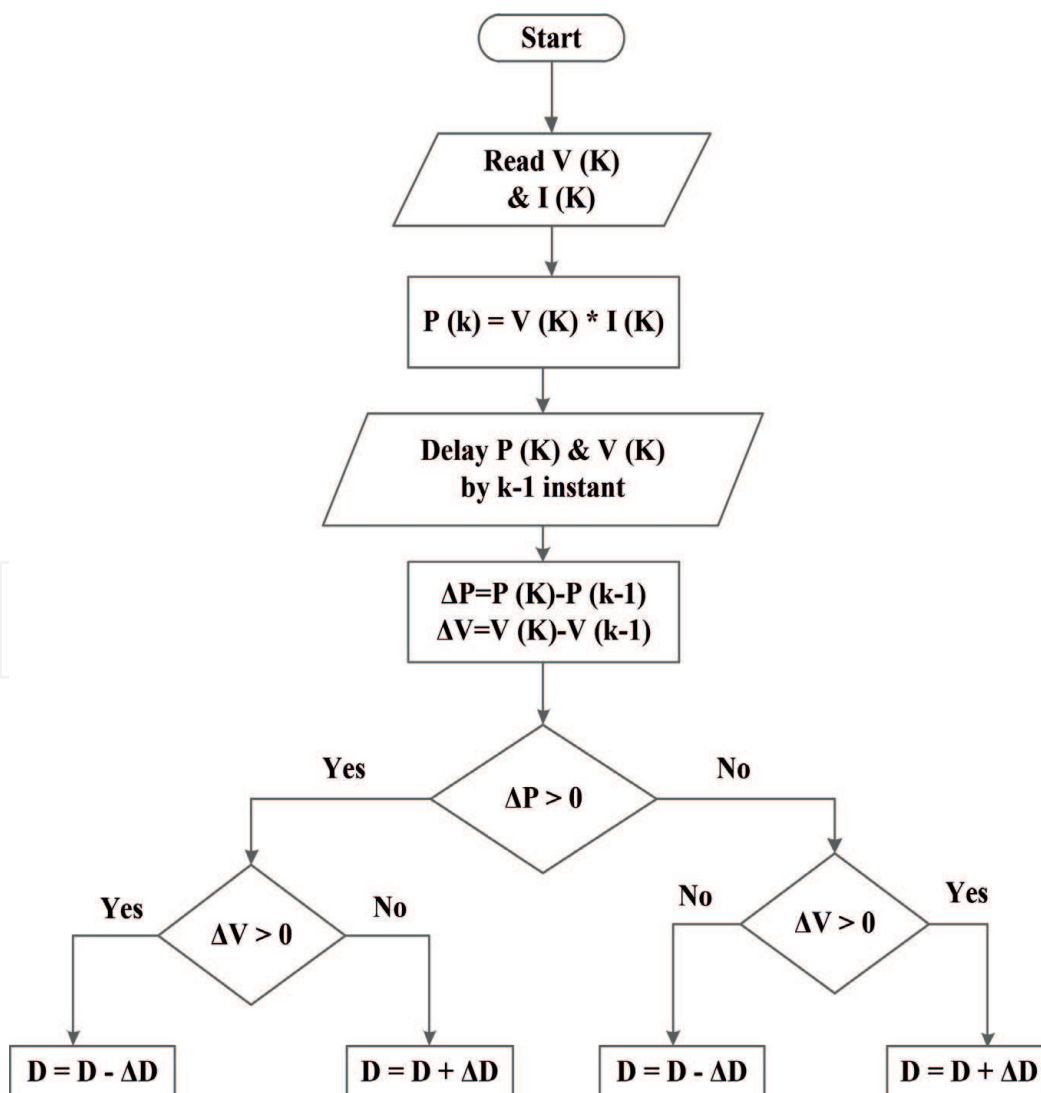


Figure 4.
 Hill climbing/perturb and observe MPPT flowchart.

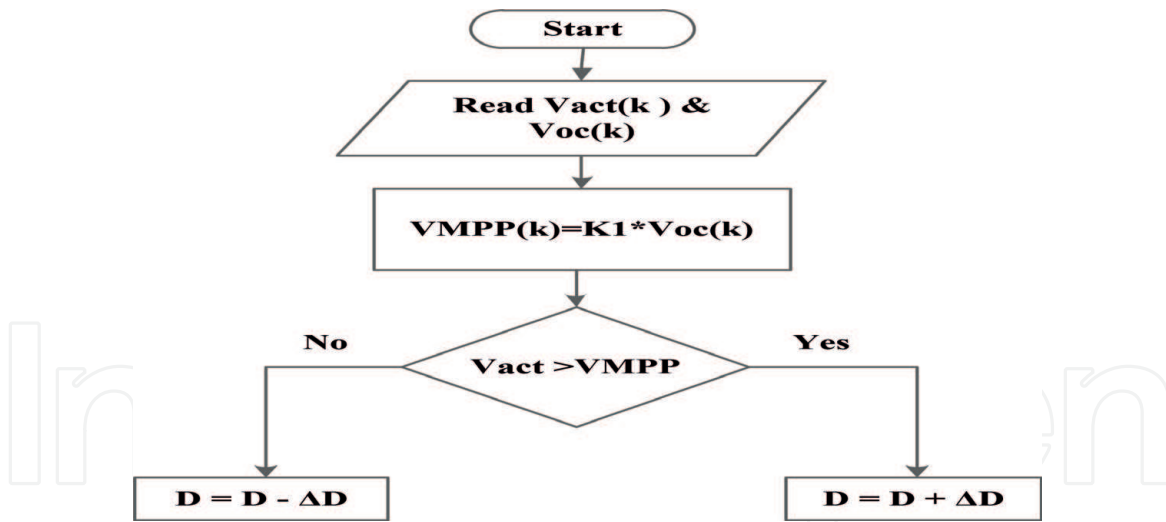


Figure 5. Fractional open-circuit voltage algorithm.

4.3 Fractional open-circuit voltage algorithm

The linear characteristic of V_{OC} under various operating conditions paves the way for FOCV based MPPTC [15, 18].

$$V_{MPP} \cong K_1 \times V_{OC} \tag{8}$$

where K_1 is a constant of proportionality which depends on the characteristics of the PV panels. The algorithm of the fractional open circuit voltage is presented in **Figure 5**. The duty cycle is reduced or increase by comparing V_{MPP} computed from V_{OC} and the actual voltage V_{act} . The factor K_1 ranges between 0.71 and 0.78.

5. Fractional order PID control

FOPID control is proven to provide more flexibility and ability to enhance modeling and control of systems' dynamics [19]. The transfer function of FOPID is given by

$$G(S) = K_p \left\{ 1 + \frac{1}{T_i s^\lambda} + T_d s^\mu \right\} \tag{9}$$

where K_p , T_i and T_d are controller gains while λ and μ are the integral and differential power in real number. By changing the values of λ and μ , the controller can be configured to behave within the four possibilities presented in **Figure 6** [20].

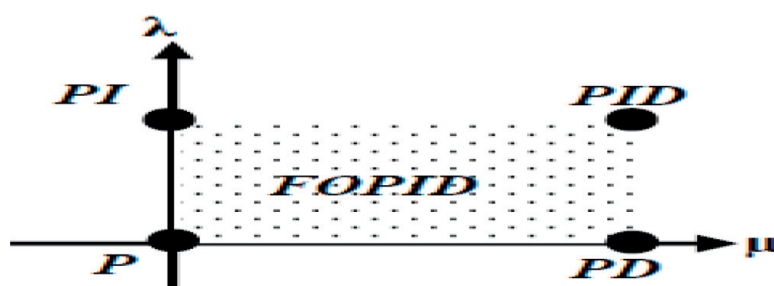


Figure 6. Control space of FOPID.

Figure 6 shows fractional PID control space. Recently, there are many optimization techniques are employed for solving engineering problems especially PI, PID, FOPI and FOPID based problems [19–39].

6. Grey wolf optimizer (GWO) technique

Grey wolves are considered as apex predators, meaning that they are at the top of the food chain [10]. **Figure 7** presents the social hierarchy of Grey wolves.

The mathematically model of the encircling behavior is represented by the following equations:

$$D = |CX_P - AX(t)| \quad (10)$$

$$X(T + 1) = X_P(t) - AD \quad (11)$$

The vectors A and C are calculated as follows:

$$A = 2A r_1 - a \quad (12)$$

$$C = 2r_2 \quad (13)$$

Note that the random vectors (r_1 and r_2) allow wolves to reach any position between the points illustrated in **Figure 8**. So a grey wolf can update its position inside the space around the prey in any random location by using Eqs. (10) and (11).

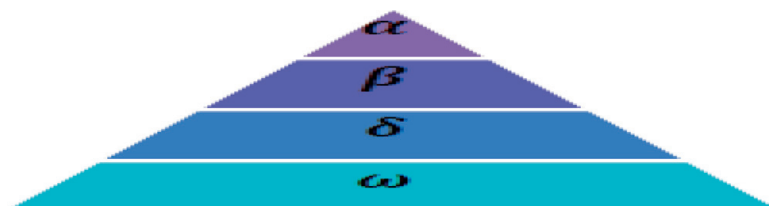


Figure 7.
 Hierarchy of grey wolf (dominance decreases from top down).

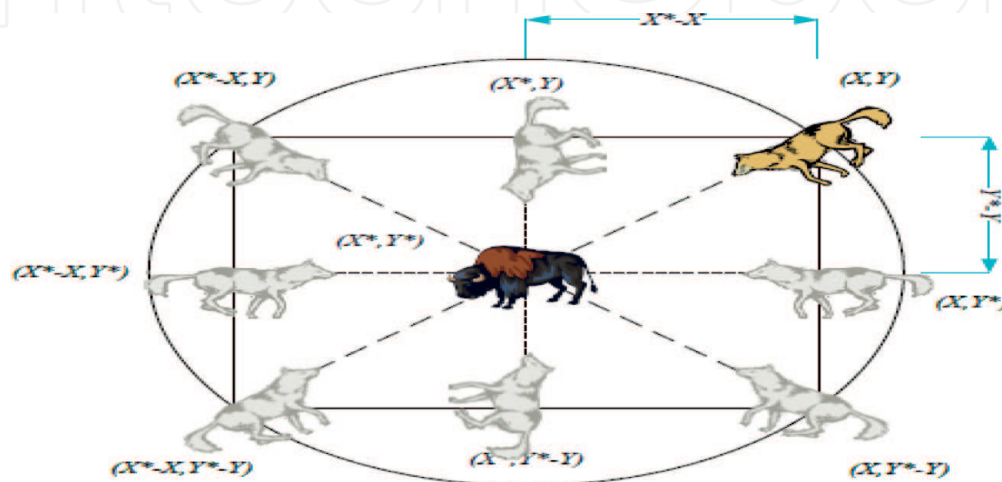


Figure 8.
 Position vectors and their possible next locations.

7. Simulation results and comparison

To validate the effectiveness of the proposed MPPTCs, the system under study quipped with only one MPPTC (P&O, Inc. Cond, FOCV, and FSOC) at a time is simulated. Wide range of operating temperature and irradiance is considered in this chapter to prove the superiority of GWO based MPPTCs over the conventional ones. The simulation results spot the light on the output voltage as well as power.

7.1 Perturb and observe method

The system equipped with P&O based MPPTC is simulated under small as well as large variations in temperature and irradiance. **Figure 9** demonstrates the dynamic response of the output voltage. The time response of the output voltage presents small voltage ripples during the rapid changes of temperature and irradiance. A proper filter can be employed to remove these ripples. In **Figure 10**, the dynamic time response for the output power is presented. The features of the time response for the system output power in case of P&O based MPPTC interprets that the P&O based MPPTC smoothly tracks MPP but with some oscillations especially at the transition intervals (high to low or low to high temperature and irradiance variations).

7.2 Incremental conductance method

The time response for the system voltage and output power is presented in **Figures 11** and **12** respectively. The dynamic response for the system output power in case of Inc. Cond based MPPTC is significantly improved compared to P&O case even in case of rapid variations in temperature and irradiance. **Figure 12** spotted the light on how Inc. Cond based MPPTC supersedes the P&O in smoothly tracking MPP.

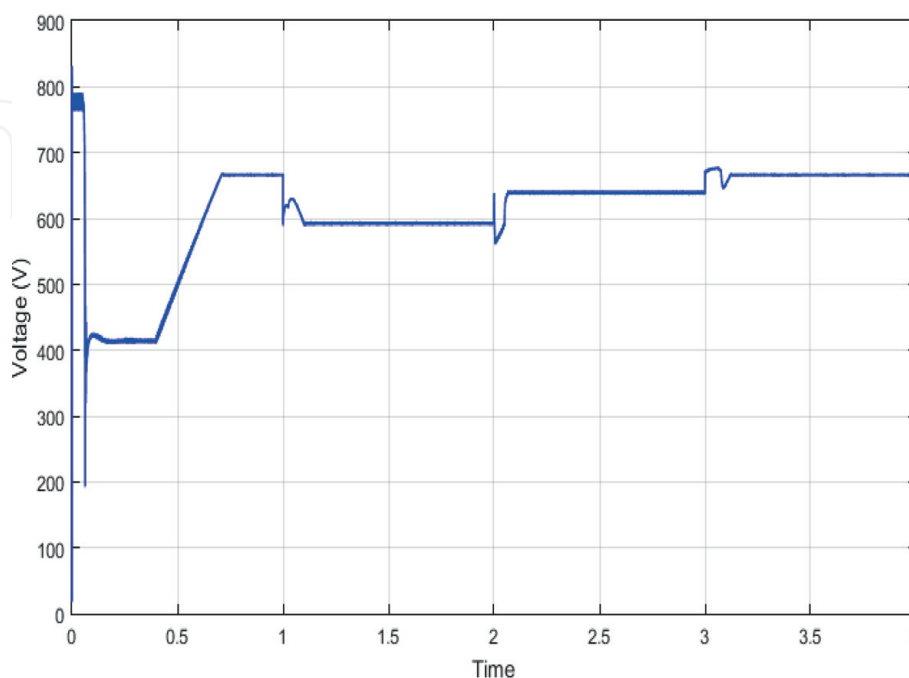


Figure 9.
P&O based MPPTC's output voltage waveform at different radiation and temperature.

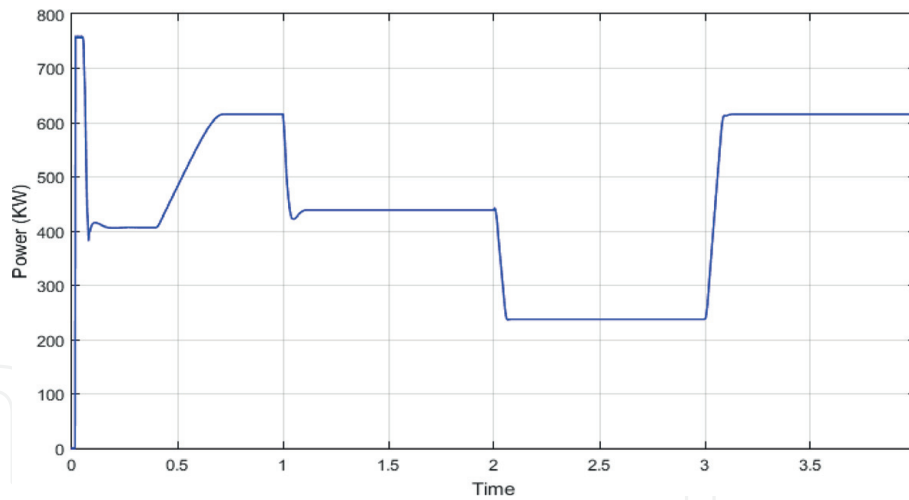


Figure 10.
P&O based MPPTC's output power waveform at different radiation and temperature.

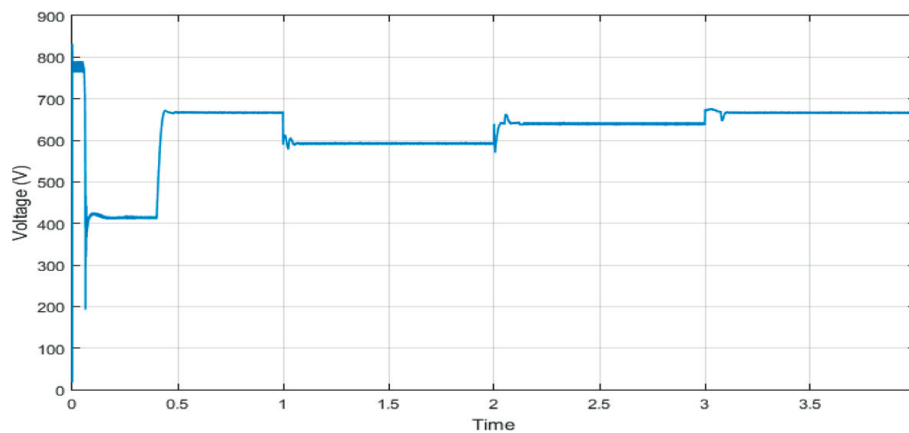


Figure 11.
Inc. Cond based MPPTC's output voltage waveform at different radiation and temperature.

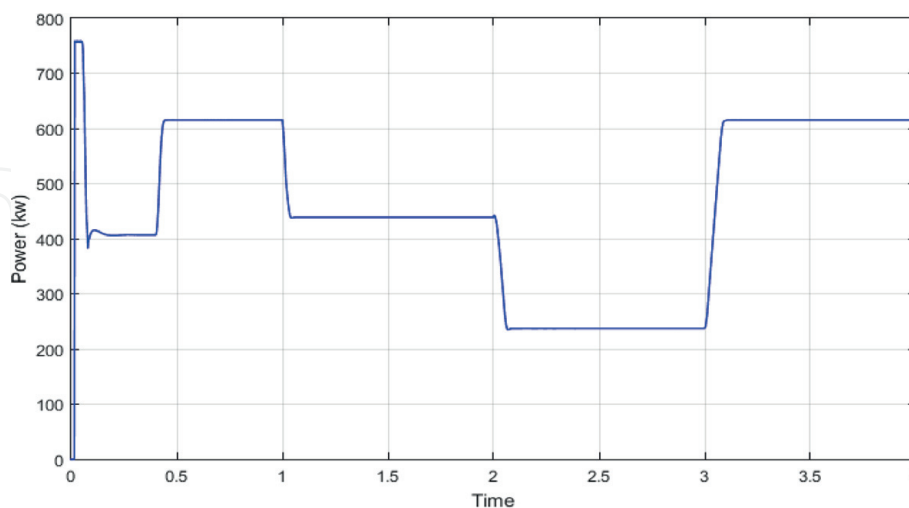


Figure 12.
Inc. Cond based MPPTC's output power waveform at different radiation and temperature.

7.3 Open-circuit voltage method

The time response of the voltage and output power for the system equipped with FOCV based MPPTC is shown in **Figures 13** and **14** respectively. It is evident from

the simulation results that the system response is poor especially in case of rapid changes in the operating conditions.

Table 1 presents a comparative study between the various applied MPPT techniques. It is worth mentioning that although Inc. Cond MPPT technique has good tracking response but it requires voltage and current measurements. Moreover, its implementation complexity is higher than P&O and fractional open circuit voltage methods.

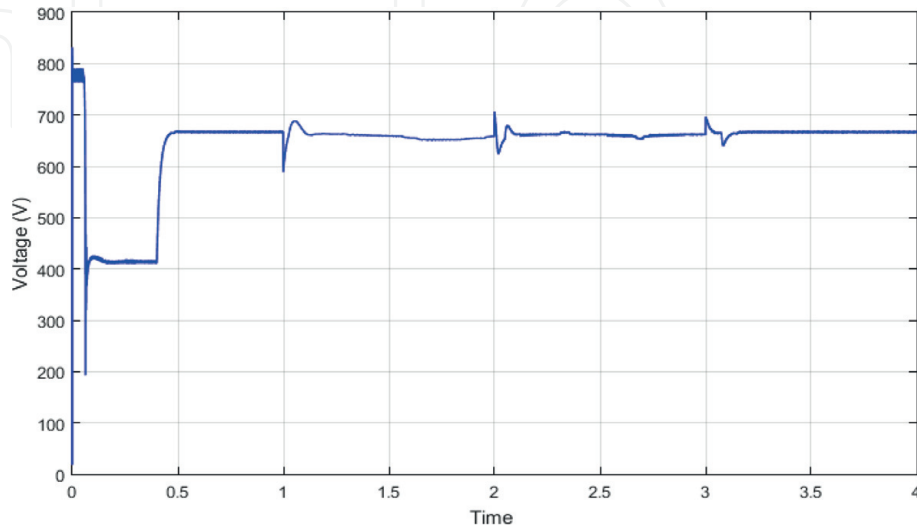


Figure 13.
FOCV based MPPTC's output voltage waveform at different radiation and temperature.

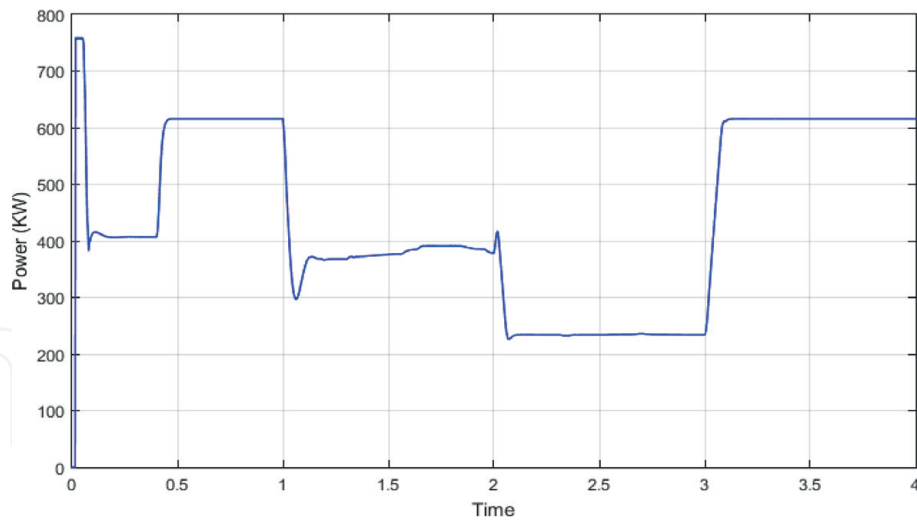


Figure 14.
FOCV based MPPTC's output power waveform at different radiation and temperature.

MPPT techniques	Parameters		
	Convergence speed	Implementation complexity	Sensed parameters
P & O method	Varies	Low	Voltage
Inc Cond method	Varies	Medium	Voltage, current
Fractional V_{oc} method	Medium	Low	Voltage

Table 1.
Comparative study for various MPPT techniques.

8. Conclusion

In this paper, four MPPT algorithms are implemented using the Boost converter. The models are simulated using MATLAB/SIMULINK. The simulation results show that P&O and Inc. Cond MPPTCs have better efficiency than FOCV and FSCC MPPTCs. Although, Inc. Cond provides good performance but its implementation has some challenges. Moreover, FOCV and FSCC based MPPTCs are very simple but both controllers lack to the accuracy due to their dependency on constant gains. Therefore, solar cell performance is significantly improved in the presence of MPPTCs. Hence, MPPTCs improvement has vital role in expanding the utilization of PV based systems.

Acknowledgements

The authors gratefully acknowledge the support of the Egyptian high education ministry, The Science and Technology Development Fund (STDF), and the French Institute in Egypt (IFE).

Conflict of interest

The authors of this chapter did not have 'conflict of interest' for publishing.

Author details


Mohamed Ahmed Ebrahim^{1*} and R.G. Mohamed²

¹ Faculty of Engineering at Shoubra, Benha University, Cairo, Egypt

² Eastern Company, Giza, Egypt

*Address all correspondence to: mohamed.mohamed@feng.bu.edu.eg

IntechOpen

© 2019 The Author(s). Licensee IntechOpen. This chapter is distributed under the terms of the Creative Commons Attribution License (<http://creativecommons.org/licenses/by/3.0>), which permits unrestricted use, distribution, and reproduction in any medium, provided the original work is properly cited. 

References

- [1] Wolfsegger C, Fraile D, Philbin P, Teske S. Solar generation-solar electricity for over one billion people and two million jobs by 2020. In: European Photovoltaic Industry Association, Renewable Energy House, Belgium and Greenpeace International, The Netherlands, Report No. 5. 2008
- [2] Mohamed RG, Ibrahim DK, Youssef HK, Rakha HH. Optimal sizing and economic analysis of different configurations of photovoltaic systems. *International Review of Electrical Engineering (I.R.E.E.)*. January–February 2014;9(1):146-156
- [3] Mohamed RG, Ibrahim DK. Optimal sizing and economic analysis of stand-alone photovoltaic system. In: *The 2012 World Congress on Power and Energy Engineering (WCPEE'12)*; Apr. Vol. 4. 2012. pp. 188-195
- [4] Renewable Capacity Statistics 2018 (IRENA). <https://www.irena.org/publications/2018/Mar/Renewable-Capacity-Statistics-2018>
- [5] Annual Report 2018 (NREA). <http://www.nrea.gov.eg/Content/reports/English%20AnnualReport.pdf>
- [6] Rekioua D, Achour AY, Rekioua T. Tracking power photovoltaic system with sliding mode control strategy. *Renewable and Sustainable Energy Reviews*. 2013:219-230
- [7] Mukhopadhyay S, Chen YQ, Singh A, Edwards F. Fractional order plasma position control of the STOR-1M Tokamak. In: *Joint 48th IEEE Conference on Decision and Control and 28th Chinese Control Conference*. 2009. pp. 422-427
- [8] Li Y, Chen Y, Ahn H-S. A generalized fractional-order iterative learning control. In: *50th IEEE Conference on Decision and Control and European Control Conference (CDC-ECC)*. 2011. pp. 5356-5361
- [9] Wang CY, Luo Y, Chen YQ. Fractional order proportional integral (FOPI) and [Proportional Integral] (FO [PI]) controller designs for first order plus time delay (FOPTD) systems. In: *Chinese Control and Decision Conference*. 2009. pp. 329-334
- [10] Mirjalili S, Mirjalili SM, Lewis A. *Advances in engineering software. Renewable and Sustainable Energy Reviews*. 2014:46-61
- [11] Khalid H, Mohamed TB, Ibrahim, Saad NB. Boost converter design with stable output voltage for wave energy. *International Journal of Information Technology and Electrical Engineering*. February 2013;2(1)
- [12] Sathya P, Natarajan R. Design and implementation of 12V/24V closed loop boost converter for solar powered LED by lighting system. *International Journal of Engineering and Technology (IJET)*. Feb-Mar 2013;5(1)
- [13] Debashis DS, Pradhan SK. *Modeling and Simulation of PV Array with Boost Converter*. Rourkela: National Institute of Technology; 2011
- [14] Hieu Nguyen X, Nguyen MP. Mathematical modeling of photovoltaic cell/module/arrays with tags in Matlab/Simulink. *Environmental System Research*. 2015;1(1):1-13
- [15] ESRAM T, Chapman PL. Comparison of photovoltaic array maximum power point tracking techniques. *IEEE transactions on Energy Conversion*. June 2007
- [16] Stamatescua I, Făgărășana I, Stamatescua G. Design and

- implementation of a solar-tracking algorithm. 24th DAAAM International Symposium on Intelligent Manufacturing and Automation, 2013. *Procedia Engineering*. 2014;**1**(1): 500-507
- [17] Femia N, Giovanni Petrone M, Spagnuolo G, Vitelli M. Optimization of perturb and observe maximum power point tracking method. *IEEE Transactions on Power Electronics*. July 2005;**20**(4):963-973
- [18] Sai Babu C. Design and analysis of open circuit voltage based maximum power point tracking for photovoltaic system. *International Journal of Advances in Science and Technology*. 2011;**2**(2):51-86
- [19] Tajjudin M, Arshad NM, Adnan R. A design of fractional-order PI controller with error compensation. *International Journal of Computer, Electrical, Automation, Control and Information Engineering*. 2013;**7**(6):727-735
- [20] Lachhab N, Svaricek F, Wobbe F, Rabba H. Fractional order PID controller (FOPID)-toolbox. In: *European Control Conference (ECC) July 17–19, Zürich*. 2013. pp. 3694-3699
- [21] Aouchiche N, Aitcheikh MS, Becherif M, Ebrahim MA. AI-based global MPPT for partial shaded grid connected PV plant via MFO approach. *Solar Energy*. 2018;**171**:593-603
- [22] Ebrahim MA, Becherif M, Abdelaziz AY. Dynamic performance enhancement for wind energy conversion system using moth-flame optimization based blade pitch controller. *Sustainable Energy Technologies and Assessments*. 2018;**27**: 206-212
- [23] Benmouna A, Becherif M, Depernet D, Ebrahim MA. Novel energy management technique for hybrid electric vehicle via interconnection and damping assignment passivity based control. *Renewable Energy*. 2018;**119**: 116-128
- [24] Maher M, Ebrahim MA, Mohamed EA, Mohamed A. Ant-lion inspired algorithm based optimal design of electric distribution networks. In: *2017 Nineteenth International Middle East Power Systems Conference (MEPCON)*; IEEE. 2017, December. pp. 613-618
- [25] Aouchiche N, Cheikh MA, Becherif M, Ebrahim MA, Hadjarab A. Fuzzy logic approach based MPPT for the dynamic performance improvement for PV systems. In: *2017 5th International Conference on Electrical Engineering-Boumerdes (ICEE-B)*. October; IEEE. 2017. pp. 1-7
- [26] Mohamed RG, Ebrahim MA, Bendary FM, Osman SAA. Transient stability enhancement for 20 MW PV power plant via incremental conductance controller. *International Journal of System Dynamics Applications (IJSDA)*. 2017;**6**(4): 102-123
- [27] Maher M, Ebrahim MA, Mohamed EA, Mohamed A. Ant-lion optimizer based optimal allocation of distributed generators in radial distribution networks. *International Journal of Engineering and Information Systems*. 2017;**1**(7):225-238
- [28] Mousa ME, Ebrahim MA, Hassan MM. Optimal fractional order proportional—integral—differential controller for inverted pendulum with reduced order linear quadratic regulator. In: *Fractional Order Control and Synchronization of Chaotic Systems*. Cham: Springer; 2017. pp. 225-252
- [29] Ebrahim MA, AbdelHadi HA, Mahmoud HM, Saied EM, Salama MM. Optimal design of MPPT controllers for

grid connected photovoltaic array system. *International Journal of Emerging Electric Power Systems*. 2016; **17**(5):511-517

[30] Mousa ME, Ebrahim MA, Hassan MM. Stabilizing and swinging-up the inverted pendulum using PI and PID controllers based on reduced linear quadratic regulator tuned by PSO. *International Journal of System Dynamics Applications*. 2015; **4**(4):52-69

[31] Jagatheesan K, Anand B, Ebrahim MA. Stochastic particle swarm optimization for tuning of PID controller in load frequency control of single area reheat thermal power system. *International Journal of Energy and Power Engineering*. 2014; **8**(2): 33-40

[32] Ebrahim MA, El-Metwally KA, Bendary FM, Mansour WM, Ramadan HS, Ortega R, et al. Optimization of proportional-integral-differential controller for wind power plant using particle swarm optimization technique. *International Journal of Emerging Technologies in Science and Engineering*. 2011

[33] Ahmed M, Ebrahim MA, Ramadan HS, Becherif M. Optimal genetic-sliding mode control of VSC-HVDC transmission systems. *Energy Procedia*. 2015; **74**:1048-1060

[34] Jagatheesan K, Anand B, Dey N, Ebrahim MA. Design of proportional-integral-derivative controller using stochastic particle swarm optimization technique for single-area AGC including SMES and RFB units. In: *Proceedings of the Second International Conference on Computer and Communication Technologies*. New Delhi: Springer; 2016. pp. 299-309

[35] Ali AM, Ebrahim MA, Hassan MM. Automatic voltage generation control for two area power system based on particle swarm optimization. *Indonesian*

Journal of Electrical Engineering and Computer Science. 2016; **2**(1):132-144

[36] Ebrahim MA, Elyan T, Wadie F, Abd-Allah MA. Optimal design of RC snubber circuit for mitigating transient overvoltage on VCB via hybrid FFT/wavelet genetic approach. *Electric Power Systems Research*. 2017; **143**: 451-461

[37] Soued S, Ebrahim MA, Ramadan HS, Becherif M. Optimal blade pitch control for enhancing the dynamic performance of wind power plants via metaheuristic optimizers. *IET Electric Power Applications*. 2017; **11**(8): 1432-1440

[38] Ebrahim MA. Towards robust non-fragile control in wind energy engineering. *Indonesian Journal of Electrical Engineering and Computer Science*. 2017; **7**(1):29-42

[39] Ebrahim MA, Ramadan HS. Interarea power system oscillations damping via AI-based referential integrity variable-structure control. *International Journal of Emerging Electric Power Systems*. 2016; **17**(5): 497-509